BNL-228357-2025-JAAM

# CO2 Adsorption and Hydrogenation on Inverse InOx/Cu(111) Catalysts: Active Role of the Oxide-Metal Interface

P. Reddy Kasala, J. A. Rodriguez

To be published in "ACS Applied Materials & Interfaces"

June 2025

Chemistry Department

**Brookhaven National Laboratory**

**U.S. Department of Energy**

USDOE Office of Science (SC), Basic Energy Sciences (BES)

# DISCLAIMER

# $CO_2$ Adsorption and Hydrogenation on Inverse $InO_x$/Cu(111) Catalysts: Active Role of the Oxide-Metal Interface

Kasala Prabhakar Reddy,[1] Hojoon Lim,[3] Arephin Islam,[1] Yi Tian,[2] Adrian Hunt,[3] Iradwikanari Waluyo,[3] and José A. Rodriguez[1, 2] *

[1]*Chemistry Division, Brookhaven National Laboratory, Upton, New York 11973 (USA)*

[2]*Department of Chemistry, Stony Brook University, Stony Brook, New York 11794 (USA)*

[3]*National Synchrotron Light Source II, Brookhaven National Laboratory, Upton, New York 11973 (USA)*

* To whom correspondence should be addressed, rodrigez@bnl.gov
Tel. 631-344-2246

## Abstract

The direct conversion of carbon dioxide ($CO_2$) into methanol via hydrogenation is essential for industrial applications. Recent studies on catalysts that contain an inverse oxide/metal configuration have shown very good catalytic performance for the $CO_2$ hydrogenation to methanol process. In this study, we investigated the behavior of indium oxide-Cu(111) interfaces under pure $CO_2$ and $CO_2/H_2$ mixtures using synchrotron-based ambient-pressure X-ray photoelectron spectroscopy (AP-XPS). Initially, a single layer of copper oxide ($Cu_xO$) was grown on the Cu(111) surface by controlled oxidation. On this surface, indium was deposited at room temperature. Oxygen atoms transferred from $Cu_xO$/Cu(111) to the indium metal upon deposition, forming In-O-Cu bonds and active interfaces. Although Cu(111) is not very active for the binding and activation of $CO_2$, the formed $InO_x$-Cu(111) interfaces had no problem adsorbing and dissociating the molecule at room temperature. Reaction of $CO_2$ with $H_2$ on $InO_x$-Cu(111) yielded surface-bound $H_3CO$, $CO_2^{\delta-}$, $CO_3$, and $CH_x$ species that are typical intermediates in the production of methanol and other oxygenates. The $InO_x$-Cu(111) interface underwent dynamic chemical changes under reaction conditions, forming In-Cu alloys at low indium coverages (< 0.05 monolayer), while at higher indium coverages a mixture of an In-Cu and $InO_x$ was detected in XPS. These findings indicate that $InO_x$/In-Cu interfaces can play a key role in processes aimed at the trapping and valorization of $CO_2$.

**Keywords:** Indium oxide – copper interfaces; Copper; Indium oxide; $CO_2$ activation; Methanol production.

## Introduction

A substantial growth of energy demand combined with climate challenges caused by excessive $CO_2$ emissions into the atmosphere have led to a general interest in the valorization of this molecule. Thus, various approaches have been adopted to achieve "carbon neutrality" including carbon capture, utilization, and storage (CCUS) technologies.[1-3] Among these, utilization of $CO_2$ as a precursor in the synthesis of methanol ($CO_2 + 3H_2 \rightarrow CH_3OH + H_2O$) is a key reaction in C1 catalysis and a vital process in the chemical industry. $CH_3OH$ is particularly advantageous, as it can be used as a direct fuel or can blend with gasoline.[4-5] Thus, the $CO_2$ hydrogenation to $CH_3OH$ process offers a promising pathway to address the growing energy demands while helping to control climate changes.

Copper-based catalysts with a Cu-ZnO-$Al_2O_3$ formulation are commonly used for producing $CH_3OH$ from syngas, and a small amount of $CO_2$ (<5 vol %) is added to the reaction mixture for enhancing the reaction rate.[6-7] When it comes to direct $CO_2$ hydrogenation to $CH_3OH$ process, the same catalyst has a limited $CO_2$ conversion that forces operation at high temperatures (500-550 K) where the selectivity for $CH_3OH$ conversion is not large (~60 %).[6-14] Thus, the development of new copper-based catalysts is essential for improving the $CO_2 \rightarrow CH_3OH$ conversion efficiency. Recently, indium oxide ($In_2O_3$)-based catalysts showed good selectivity for $CH_3OH$ under moderate $CO_2$ hydrogenation conditions. Both theoretical and experimental studies suggest that oxygen vacancies on the $In_2O_3$ surface play an important role in activating $CO_2$ and $H_2$, and in promoting $CH_3OH$ synthesis.[8-10] Further deposition of metals (Pd, Au, Ir, Pt, Rh, Ni, Ag, and Cu) onto the $In_2O_3$ surface creates metal-oxide interfaces that enhance $H_2$ dissociation and the overall hydrogenation capacity of the catalytic system.[11-12] Notably, the deposition of non-expensive metals, such as copper (Cu), on the $In_2O_3$ surface offers a promising approach for improving process efficiency.[13] According to previous works in the literature, the Cu/$In_2O_3$ catalyst exhibits excellent $CH_3OH$ selectivity (~ 90%) in $CO_2$ hydrogenation.[13, 15-16] In spite of substantial research, it is not well known the intrinsic reactivity of Cu-$InO_x$ interfaces towards $CO_2$ and $CO_2/H_2$ mixtures. Over-reduction of $InO_x$-Cu interfaces by hydrogen could lead to the generation of Cu–In alloy phases with distinctive chemical and catalytic properties.[17]

In heterogeneous catalysis, inverse oxide/metal systems are receiving a lot of attention as catalysts for the valorization of $CO_2$[12, 18-21] and perhaps are the best approach to understand the links between structure, chemical composition, and reaction mechanism.[21-23] In simple terms, their

interface contains oxide nanostructures in contact with a metal component.[22-23] These types of systems often display higher levels of catalytic activity compared to traditional metal/oxide catalysts as reactants can easily be accessible to active sites involving the oxide. In addition, conventional $Cu/ZnO/Al_2O_3$ catalysts show a ZnO overlayer on Cu particles during $CO_2$ hydrogenation to $CH_3OH$, suggesting that an inverse oxide/metal catalyst configuration is a likely active phase.[24] Indeed, the addition of ZnO nanostructures to Cu(111) or Cu(100) produces very active systems for the binding and valorization of $CO_2$.[25-27] Hence, here we used synchrotron-based ambient-pressure X-ray photoelectron spectroscopy (AP-XPS) to study the intrinsic chemistry of $CO_2$ and $CO_2/H_2$ mixtures on interfaces generated by the deposition of $InO_x$ on Cu(111). The article is organized as follows: First, we will examine the formation of $InO_x$ overlayers on the copper substrate, and then we will describe systematic studies for reaction of the oxide-metal interfaces with $H_2$, $CO_2$ and $CO_2/H_2$ mixtures. It is shown that these interfaces have a unique chemical behavior not seen for pure copper or indium oxide.

**Experimental Section**

Ambient pressure X-ray photoelectron spectroscopy (AP-XPS) experiments were carried out at the 23-ID-2 (IOS) beamline of the National Synchrotron Light Source-II (NSLS-II) at Brookhaven National Laboratory, USA. The detailed specifications and performance of this beamline was previously discussed elsewhere.[28] The XPS spectra of C 1*s* and Cu 2*p* regions were collected using photon energies of 380 and 1142 eV, respectively, while In 3*d*, In MNN, and O 1*s* regions were collected at 760 eV photon energy. All spectra were acquired with a step size of 0.05 eV. Obtained spectra were calibrated using the Cu Fermi edge in the valence band for each photon energy.

The Cu(111) crystal was cleaned by continuous cycles of $Ar^+$ ion sputtering ($2\times10^{-5}$ Torr of Ar gas, 1 keV, 20 min, 300 K) and UHV annealing (850 K, 10 min). These cycles were repeated until the carbon and oxygen peaks had completely disappeared from the C 1*s* and O 1*s* region. A single layer of copper oxide ($Cu_xO$) was grown on the Cu(111) surface by exposing it to $1\times10^{-6}$ Torr of $O_2$ at 600 K for 20 minutes, followed by cooling to 300 K in the same oxygen background. Various coverages of $InO_x$ nanostructures were deposited on the pristine copper oxide at 300 K using a SPECS EBE-4 e-beam evaporator, and coverages were estimated using XPS. Initially, the $In/Cu_xO/Cu(111)$ surface was pretreated under $1\times10^{-6}$ Torr of $O_2$ at 600 K for 20 minutes to facilitate the full oxidation of indium, followed by exposure to 750 mTorr of $H_2$ at 400 K for 10

minutes to remove the copper oxide and produce $InO_x$/Cu (111) surfaces.

$CO_2$ was gradually introduced to the generated $InO_x$-Cu interfaces at 300 K with increasing pressure ($1\times10^{-6}$ Torr, 1 mTorr, 10 mTorr, 50 mTorr, 100 mTorr and 250 mTorr), followed by a stepwise rise of the temperature (i.e., 300 K, 400 K, and 500 K). XPS spectra of the Cu 2*p*, In 3*d*, In MNN Auger, O 1*s* and C 1*s* regions plus the valence band were acquired at each stage. Finally, 750 mTorr of $H_2$ were added to the 250 mTorr of $CO_2$ at 300 K to perform the $CO_2$ hydrogenation experiments across the temperature range of 300 to 500 K.

## Results

### A. $InO_x$ formation on a $Cu_xO$/Cu(111) surface

Overlayers of indium oxide were generated on Cu(111) to eventually examine the reaction of $H_2$, $CO_2$ and $CO_2/H_2$ mixtures with $InO_x$-copper interfaces. Initially, the Cu(111) crystal was oxidized with $1x10^{-6}$ Torr of $O_2$ at 600 K for 20 minutes, followed by a cool down to 300 K in the same oxygen environment. This led to the formation of a single-layer of copper oxide ($Cu_xO$) on the surface.[29] On the $Cu_xO$/Cu(111) surface, In metal was vapor-deposited under UHV conditions at 300 K. Figure 1 shows the XPS spectra of In 3*d* and In MNN Auger for the 0.035 and 0.32 ML of indium deposited on the $Cu_xO$/Cu(111) surface (black), and after oxidation with $1x10^{-6}$ Torr of $O_2$ at 600 K for 20 minutes (red). The 0.035 ML of Indium (black) shows the In 3*d* spectrum with a mixture of In metal (443.8 eV) and the $InO_x$ phase.[30] The corresponding In MNN region shows a broad spectrum ranging from 409-412 eV in kinetic energy, confirming the formation of $InO_x$ which co-exist with In metal on the surface. These peak positions are consistent with those reported in the literature.[11-12, 30] Formation of $InO_x$ indicates the oxygen atom being transferred from the $Cu_xO$/Cu(111) surface to the Indium metal, forming In-O-Cu bond. Cu 2*p* spectra (Figure S1a) show a slight decrease in intensity after indium deposition that attenuates the signal from the $Cu_xO$/Cu(111) system. The In/$Cu_xO$/Cu(111) surface was further treated with $1x10^{-6}$ Torr of $O_2$ at 600 K for 20 minutes to maximize the oxidation of indium on the surface,

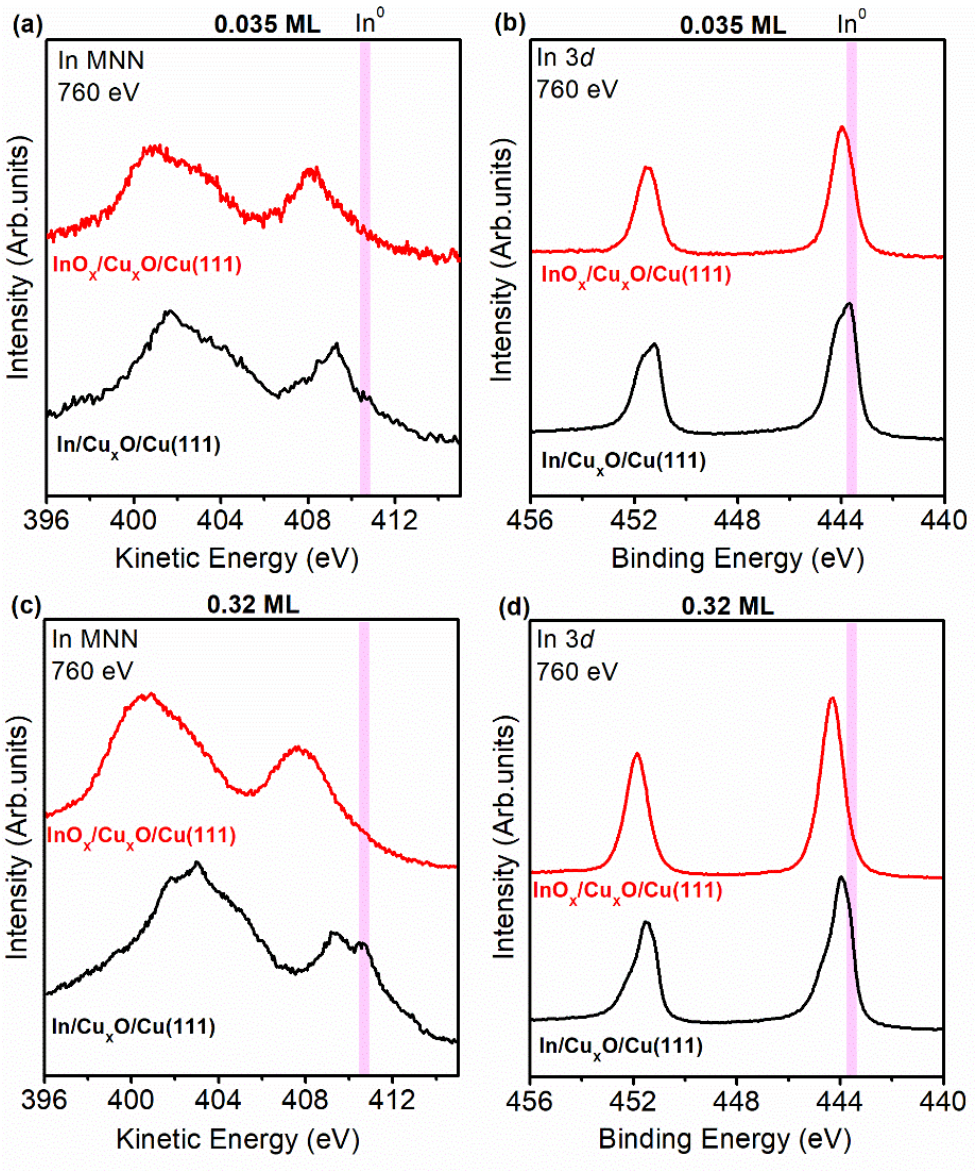


**Figure 1.** Photoemission spectra of the In MNN Auger (a, c) and In 3*d* core-level (b, d) regions for 0.035 (top panels) and 0.32 ML (bottom panels) of indium deposited on $Cu_xO$/Cu(111). The black traces correspond to the plain deposition of In at room temperature, while the red traces are for subsequent exposure to $1x10^{-6}$ Torr of $O_2$ at 600 K for 20 minutes. All the displayed XPS spectra were collected under UHV at 300 K.

as most In-based catalysts are being used in the form of $In_2O_3$ for $CO_2$ hydrogenation.[31-32] A lower binding energy hump seen for Indium metal (448.3 eV) in the In 3*d* spectra (Figure 1b,d black traces) completely disappeared, and in the In MNN spectra a peak appeared at 408 eV in kinetic energy, indicating the presence of partially oxidized indium. The valence band spectra (Fig. S1b) of the clean Cu(111) surface shows the 3*d* valence band features between binding

energies of 2 to 4 eV with a distinct $E_F$ (grey color). After oxidizing the Cu(111) surface, a new valence band feature develops at 1.7 eV, which is characteristic of $Cu_2O$ ($Cu^{1+}$) (blue color).[33] Indium deposition (black) and further oxidation did not cause any significant changes in the valence band spectrum (red).

An increase of In coverage to 0.32 ML leads to the formation of both In metal and $InO_x$ phases, as observed in In 3*d* (Figure 1c) and In MNN (Figure 1d) spectra. The Cu 2*p* spectrum intensity (Figure S1b) decreased with increase of In coverage. After oxidation, the Indium becomes more oxidized, and the extent of oxidation increases with increase of In coverage. Notably, an increase in intensity of In 3*d* (Figure 1c) and In MNN (Figure 1d) spectra and decrease of Cu 2*p* intensity (Figure S1c), suggests a redistribution of indium on the surface, forming more dispersed particles. A similar phenomenon has been seen for the $InO_x/TiO_2$ surface.[34] The typical valence band feature seen for $Cu^{1+}$ in $Cu_xO$/Cu(111) decreased (Fig. S1d) at 0.32 ML coverage, confirming the oxygen atom transfer from $Cu_xO$/Cu(111) to Indium. Further oxidation of the $InO_x/Cu_xO$/Cu(111) surface regenerate the $Cu^{1+}$ valence band feature (Fig.S1d, red).

In Figure 2, the O 1*s* spectra of the $Cu_xO$/Cu(111) surface show an asymmetric peak, resulting from contributions of both surface ($O_S$) and lattice oxygen ($O_L$) atoms, as observed in previous reports.[29] Upon indium deposition, spectra in the middle of the panels in Figure 2, oxygen atoms were transferred from the $Cu_xO$/Cu(111) substrate to indium, in agreement with the oxidation of indium seen in Figure 1. In general, features that contained In-O or In-O-Cu units appeared in the range of 529.5 to 531.5 eV. They reflect systems with different In/O stoichiometries as seen in the case of $InO_x$/Au(111).[30] A peak around 531.3-531.5 eV was observed in the MgO/Cu(111) system.[35] Further, oxidation of the In/$Cu_xO$/Cu(111) surface (top spectra in Figure 2) led to dominant features observed between 529.5 and 530.5 eV, attributed to a mixture of $Cu_xO$/Cu (111) and $InO_x/Cu_xO$/Cu(111).

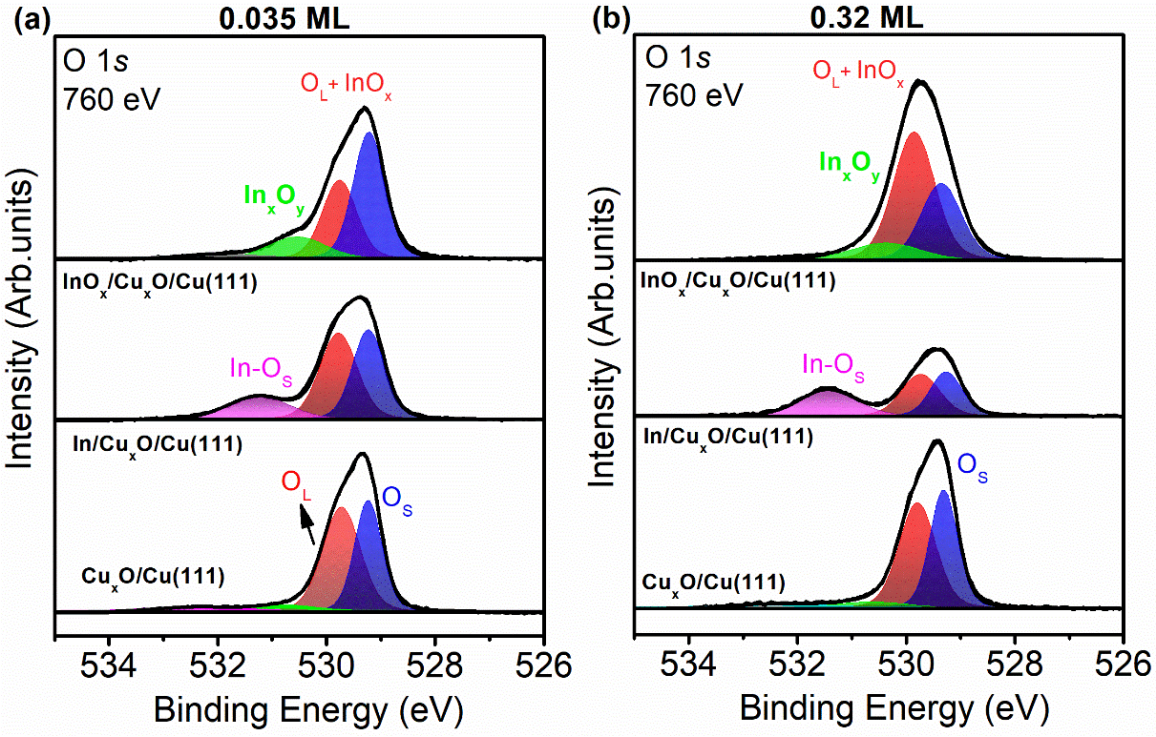


**Figure 2.** XPS spectra of O 1*s* core levels for $Cu_xO/Cu(111)$ (bottom), after 0.035 (a) and 0.32 ML (b) of indium deposition on $Cu_xO/Cu(111)$ (middle), and after oxidation with $1x10^{-6}$ Torr $O_2$ at 600 K (top). All the displayed XPS spectra were collected under UHV at 300 K.

### B. Reduction with $H_2$ of $InO_x/Cu_xO/Cu(111)$

Indium oxide-based catalysts for $CO_2$ hydrogenation are usually activated by pre-treatment in $H_2$ at elevated temperatures (400-500 K).[8-12,36] Thus, as-prepared $InO_x/Cu_xO/Cu(111)$ surfaces were pretreated with 750 mTorr of $H_2$ at 400 K. Figure 3 displays typical results for the In 3*d* and In MNN regions, before and after $H_2$ treatment. A slight positive shift in binding energy and an increase in intensity of the In 3*d* spectrum were observed. Interestingly, the Cu 2*p* spectrum (Figure S2a and S2c) also showed an increase in intensity after reduction, which implies that oxygen atoms were removed from both the In and Cu sites. A similar phenomenon was observed for the reduction of the $CeO_x/CuO_x/Cu(111)$ system[37] and $CeO_2/CuO$ powders, [38] where the hydrogen reduced the copper oxide and also removed oxygen from the ceria overlayer. In Figure 4, the H-induced chemical changes were more pronounced at lower indium coverage (0.035 ML) than at higher coverage (0.32 ML). This may reflect a reduction in the structural stability of the $InO_x$ when their size decreases.[30]

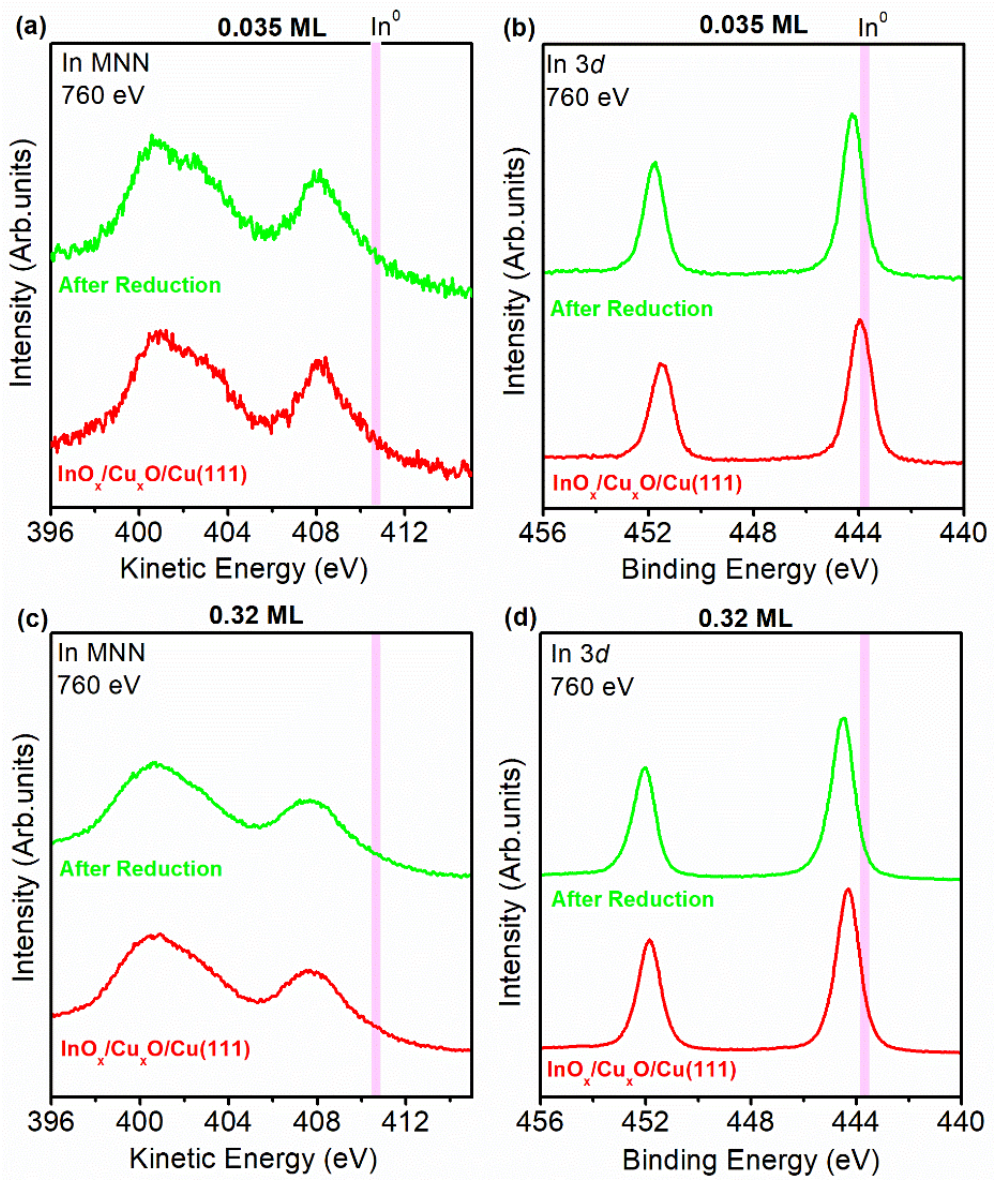


**Figure 3.** XPS spectra of In MNN (a, c) and In 3*d* (b, d) core levels for 0.035 and 0.32 ML of $InO_x/Cu_xO/Cu(111)$ (Red), and after reduction at 750 mTorr of $H_2$, 400 K for 10 min (Green). All the displayed XPS spectra were collected under UHV at 300 K.

The corresponding O 1*s* spectra (Figure 4) show a reduction in the peak intensity at ~529.1 eV (blue trace, $O_S$), which comes from the removal oxygen bound to copper due to the formation of water.[29] $H_2$ is probably dissociating on the $InO_x$ islands and then spilling to the copper oxide to form water.[29] Nevertheless, a small fraction of the copper oxide is not reduced by $H_2$. This is likely due to the presence of stable In-O-Cu units on the surface. In contrast, no large changes in the amount of O bound to Indium were seen after reduction. This is expected since CuO ($\Delta H_f^\circ$ = -56.06 kJ/mol) or $Cu_2O$ ($\Delta H_f^\circ$ = -170.71 kJ/mol) are thermodynamically less stable than the

$In_2O_3$ ($\Delta H_f^\circ$ = -923.5 kJ/mol) under standard conditions.[39-40] A noticeable hydroxide peak (~532 eV)[41] was also seen after $H_2$ treatment at lower coverages. In the case of the $Cu_xO$/Cu(111) surface with the higher indium coverage (0.32 ML), reaction with hydrogen induces a redistribution of the O species on the surface that is probably mediated by the generation of OH groups. The O purely bonded to copper decreases ($O_s$), but other species in which O also interacts with In sites and H increase in intensity. As we will see below, this is consistent with the idea of a dynamic interface that can change as a result of variations in the chemical environment.

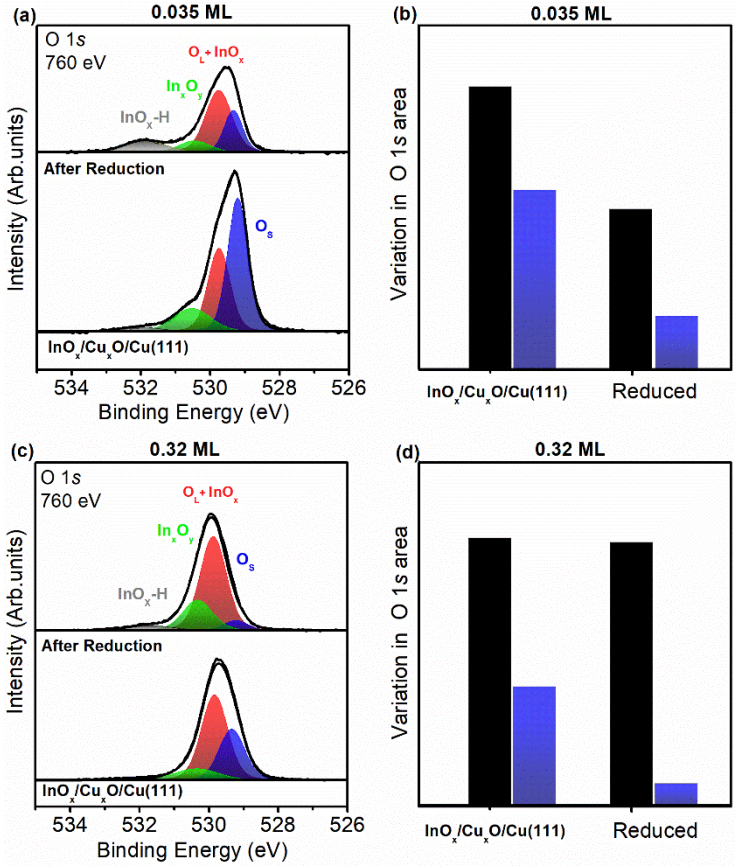


**Figure 4.** XPS spectra of O 1*s* core levels (a, c) and corresponding O 1*s* peak area variation (b, d) for 0.035 and 0.32 ML of $InO_x/Cu_xO$/Cu(111) (bottom) and after reduction at 750 mTorr $H_2$, 400 K for 10 min (up). The black color bars (b, d) represent the total amount of oxygen present on the surface and the blue color bars (b, d) correspond to the oxygen present only on the copper. All the displayed XPS spectra were collected under UHV at 300 K.

### C. Reaction with $CO_2$ of reduced $InO_x/Cu_xO$/Cu(111)

Cu(111) reacts poorly with carbon dioxide.[25-27] A minor amount of $CO_2$ dissociates on defect sites of this copper surface.[25-27] The deposition of $InO_x$ leads to a big enhancement in chemical reactivity. The reduced $InO_x/Cu_xO$/Cu(111) surfaces, shown in Figures 3 and 4, were

gradually exposed to varying partial pressures of $CO_2$ at room temperature. C 1*s* and O 1*s* spectra were collected to track $CO_2$ chemisorption and the formation of possible surface-bound species following $CO_2$ dissociation on the $InO_x/Cu_xO/Cu(111)$ surfaces. The 0.32 ML coverage (Figure 5) shows pressure-dependent $CO_2$ dissociation at room temperature. At lower pressures ($1\times10^{-6}$ Torr), $CO_2$ dissociation predominantly produced C 1*s* peaks at 284.4 and 285.1 eV, attributed to adsorbed carbon (C*) and a small amount of $CH_x$ bonded to $InO_x$ or Cu, respectively.[30, 42] These adsorbates were produced by the reactions:

$$CO_2(gas) \rightarrow C^* + 2O^* \quad (1)$$

$$C^* + xH^* \rightarrow CH_x^* \quad (2)$$

Reaction (1) clearly dominated and the H adatoms for reaction (2) were probably produced during the pre-reduction of the sample or by dissociation of $H_2$ molecules from the background gas. At higher $CO_2$ pressures (1 mTorr and above), additional peaks were observed at 283.3, 287.2, 288.6, and 289.1 eV, likely due to formation of C*/Cu, methoxy, $CO_2^{\delta-}$, and $CO_3^{2-}$ species, respectively.[43, 44] The source of hydrogen for methoxy formation, expected near a binding energy of 287 eV, [45-47] could again be coming from background $H_2$ gas or H adatoms generated during the pre-reduction process.

$$CO_2(gas) \rightarrow CO^* + O^* \quad (3)$$

$$CO^* + 3H^* \rightarrow CH_3O^* \quad (4)$$

In general, $CO_2$ adsorption on the Cu(111) surface resulted in an intense, negatively charged chemisorbed $CO_2^{\delta-}$ peak seen in both the O 1s and C 1*s* regions.[44] However, on the 0.32 ML $InO_x/Cu_xO/Cu(111)$ surface, these peaks were significantly reduced. Instead, carbonate species formed on the surface, suggesting that $CO_2$ directly interacts with lower-coordinated surface oxygen atoms, leading to carbonate formation. Upon further increasing of $CO_2$ pressure to 250 mTorr and subsequent evacuation, the $CO_2$ dissociation products intensity remained unchanged.

In Figure 5b, the O 1*s* spectra showed a peak around 529.9-529.7 eV, corresponding to both $InO_x$ and lattice oxygen from $Cu_xO$ ($O_L$). A small peak around 529.3 eV (dark blue peak), attributed to surface oxygen atoms from $Cu_xO$ was also observed.[29] The intensity of this peak increased with rising $CO_2$ pressure, indicating the oxidation of the Cu surface at room temperature by oxygen atoms coming from $CO_2$ dissociation. At higher $CO_2$ pressures, additional peaks ~530.3 eV and 531.3 eV appeared, corresponding to $In_xO_y$ and a mixture of $CH_3O^*$, $CO_2^{\delta-}$, $CO_3^*$

species, respectively. Figures S3 and S4 show the corresponding In 3*d*, In MNN, and Cu 2*p* spectra, respectively. The fact that the green trace for O atoms in $In_xO_y$ drops in intensity indicates that $CO_2$ is probably reacting with these centers to generate methoxy and carbonate-like species. Desorption of C-containing species at 500 K, Figure S5, led to an increase in the green trace for $In_xO_y$. As in the case of reaction with $H_2$, Figure 4c,d, such a behavior reflects a dynamic interface which responds to changes in the chemical environment and temperature.

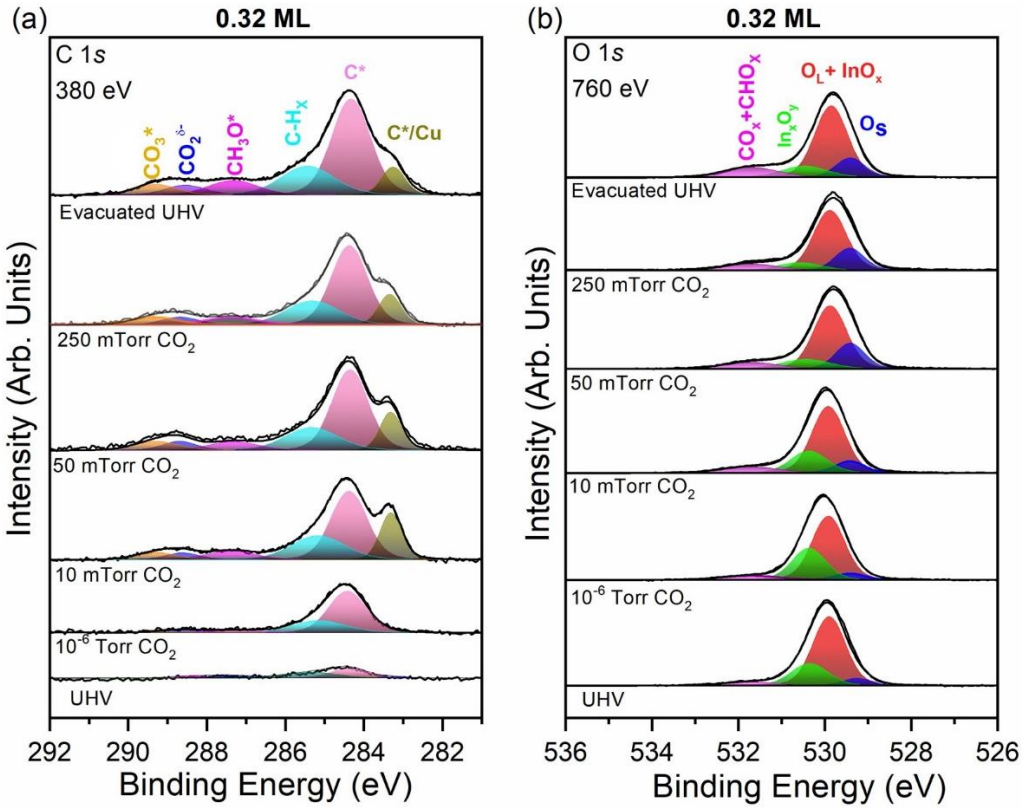


**Figure 5.** AP-XPS spectra of the (a) C 1*s* and (b) O 1*s* core levels for a 0.32 ML $InO_x/Cu_xO/Cu(111)$ surface under various partial pressure of $CO_2$ at 300 K. In a preliminary step, the sample was reduced in $H_2$ at 400 K (Figures 3 and 4).

Reintroducing 250 mTorr of $CO_2$ at 300 K (Figure 6a, bottom) had no effect on the spectra, which remained like in the evacuated case (Figure 5, top). A stepwise increase in sample temperature i.e., 300, 400, 500 K, under 250 mTorr of $CO_2$ led to removal of C*, $CH_x$, C*/Cu, methoxy, $CO_2^{\delta-}$, and $CO_3^{2-}$ species from the surface. The $C^*$ probably reacted with O from dissociated $CO_2$. Interestingly, the $CH_x$ species exhibited greater stability compared to the other species and desorbed to a lesser extent. Similarly, the O 1*s* spectrum showed a decrease in the

peak at 531.3 eV, corresponding to a reduction in formate, $CO_2^{\delta-}$, $CO_3^{2-}$ species. No changes were seen in the indium oxidation state (Figure S5).

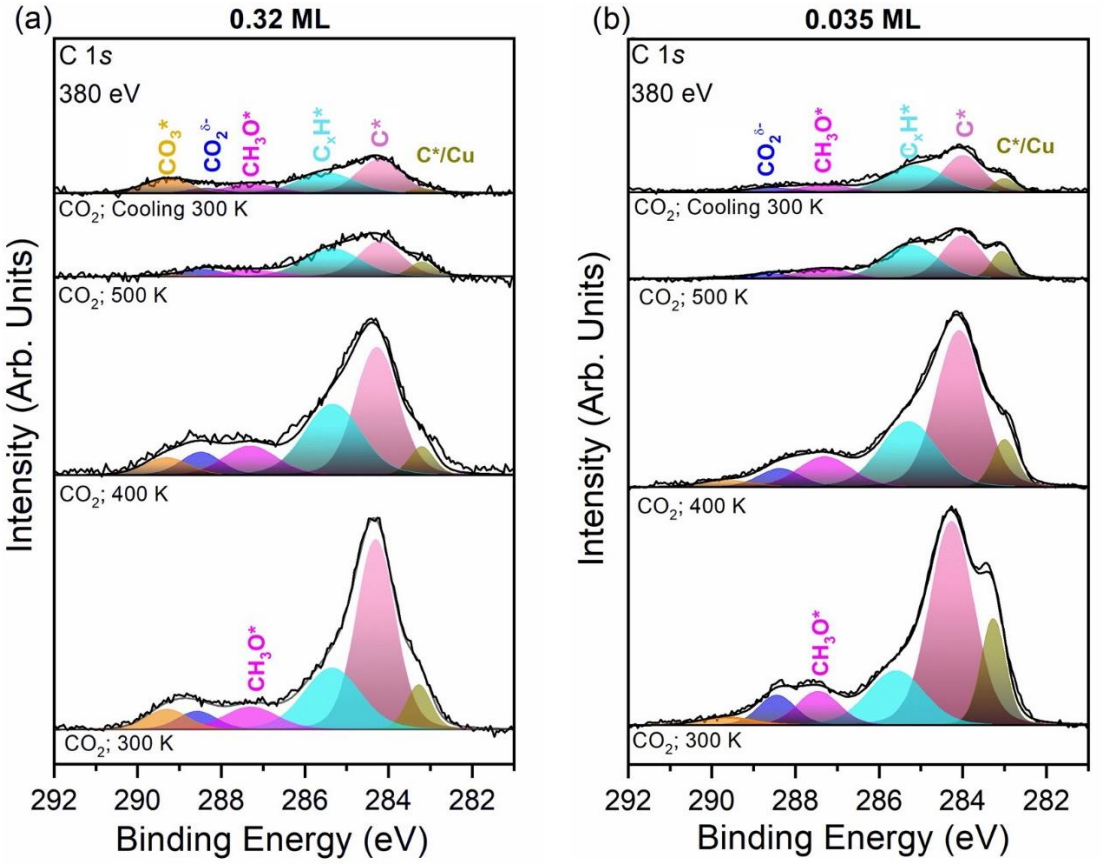


**Figure 6.** C 1*s* AP-XPS spectra collected for $InO_x/Cu_xO/Cu(111)$ surfaces with 0.32 (a) and 0.035 ML (b) of $InO_x$ under 250 mTorr of $CO_2$ at various temperatures.

Figure 6 compares the trends observed for the dissociation of $CO_2$ on $InO_x/CuOx/Cu(111)$ surfaces with 0.32 and 0.035 ML of indium oxide. More AP-XPS data for the interaction of $CO_2$ with the surface with 0.035 ML of $InO_x$ are shown in Figures S8-S13. On both surfaces, exposure to $CO_2$ resulted in the formation of C*/Cu, C*, $CH_x$, $CH_3O$ and $CO_2^{\delta-}$species.[30, 42-47] Interestingly, a somewhat more prominent C*/Cu peak was observed on the 0.035 ML $InO_x/Cu_xO/Cu(111)$ surface when compared to the 0.32 ML $InO_x/Cu_xO/Cu(111)$ surface. In contrast, the amount of carbonate formed on the surface with 0.035 ML of $InO_x$ was negligible. As we will see below, the $InO_x$-Cu interfaces of these systems responded in a different way to $CO_2/H_2$ mixtures.

### D. Reaction of $CO_2$ and $H_2$ mixtures with $InO_x/Cu_xO/Cu(111)$: Dynamics of the interface

**composition**

The pre-reduced $InO_x/Cu_xO/Cu(111)$ surfaces were exposed to $CO_2/H_2$ mixtures (1:3 ratio as in $CH_3OH$ synthesis) at temperatures ranging from 300 to 500 K. As discussed above, dosing 250 mTorr of $CO_2$ on the 0.32 ML $InO_x/Cu_xO/Cu(111)$ surface led to $CO_2$ dissociation, forming various surface species (bottom of Figure 7). Introducing 750 mTorr of $H_2$ at 300 K produced more C* (~284.2 eV), $CH_x$ (~285 eV), $CH_3O$ (~287 eV), and $CO_3^{2-}$ (289.5 eV) species in the C 1*s* region. [30, 42-47,] The increased peak at 531.5 eV in the O 1*s* region supports the formation of more $CH_xO^{\delta-}$, and $CO_3^{2-}$ species on the surface. In addition, a slight decrease in the intensity of the $Cu_xO$ peak at 300 K suggests that hydrogen atoms activated on the surface remove part of this oxide.

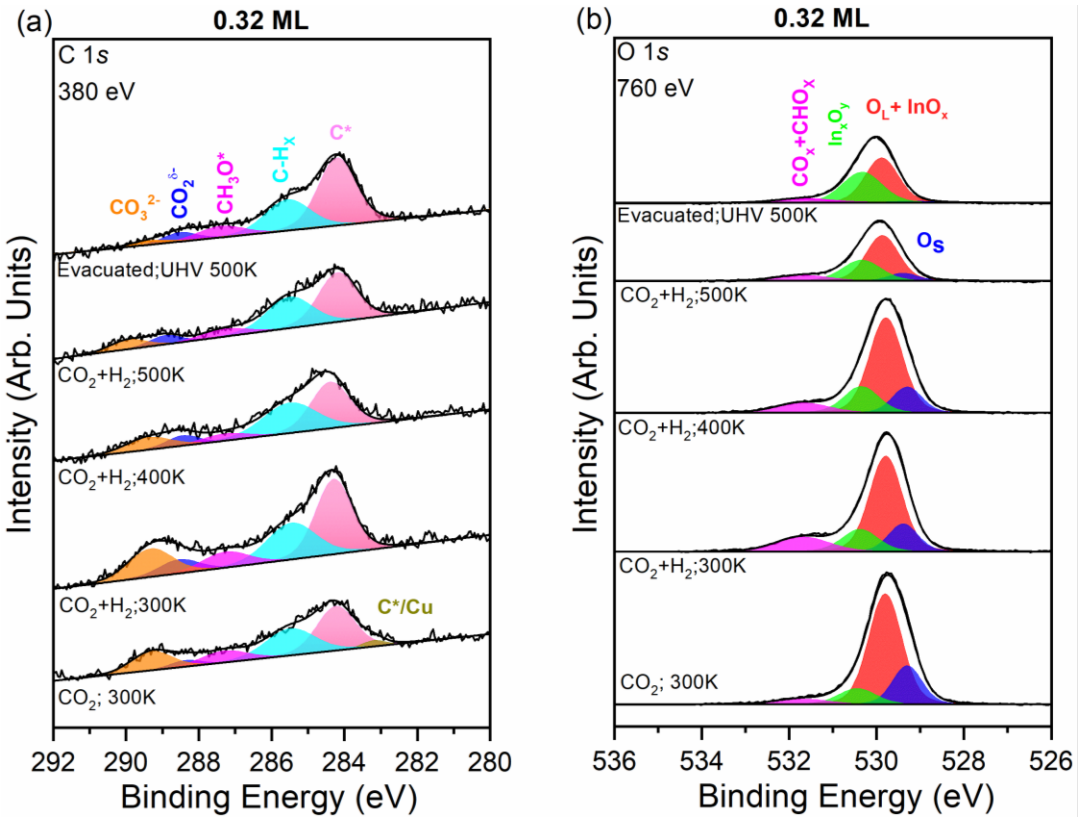


**Figure 7.** AP-XPS spectra of the (a) C 1*s* and (b) O 1*s* core levels for a 0.32 ML of $In/Cu_xO/Cu(111)$ surface under 250 mTorr of $CO_2$ and 750 mTorr of $H_2$ at various temperatures. In preliminary steps, the sample was initially reduced in $H_2$ at 400 K for 10 minutes (Figure 3) and after that treated with $CO_2$ at various temperatures (Figure 6).

Further increasing the temperature to 400 K caused a significant decrease of formate, $CO_2^{\delta-}$, and $CO_3^{2-}$ species, while the $CH_x$ and C* species remained relatively stable on the surface. This effect is more dominant at 500 K,[8-12] a typical temperature used for $CO_2$ hydrogenation using $Cu\text{-}In_2O_3$

catalysts. At this temperature, the $Cu_xO$ phase is completely reduced to copper metal (Figures 7b, Fig. S14). Indium oxide also further reduced, yielding a mixture of both In metal and $InO_x$ (Figure 8) near the copper substrate. These results point to the existence of a dynamic interface that varies composition depending on temperature and chemical environment. At medium temperatures (< 450 K), the oxidizing power of $CO_2$ wins and the indium is present as $InO_x$. An increase in temperature accelerates reduction by hydrogen and now the interface contains $InO_x$ and an alloy of indium and copper. Adsorbed, C* (284.2 eV) and $CH_x$ (285 eV) species remained present on the surface at 500 K.

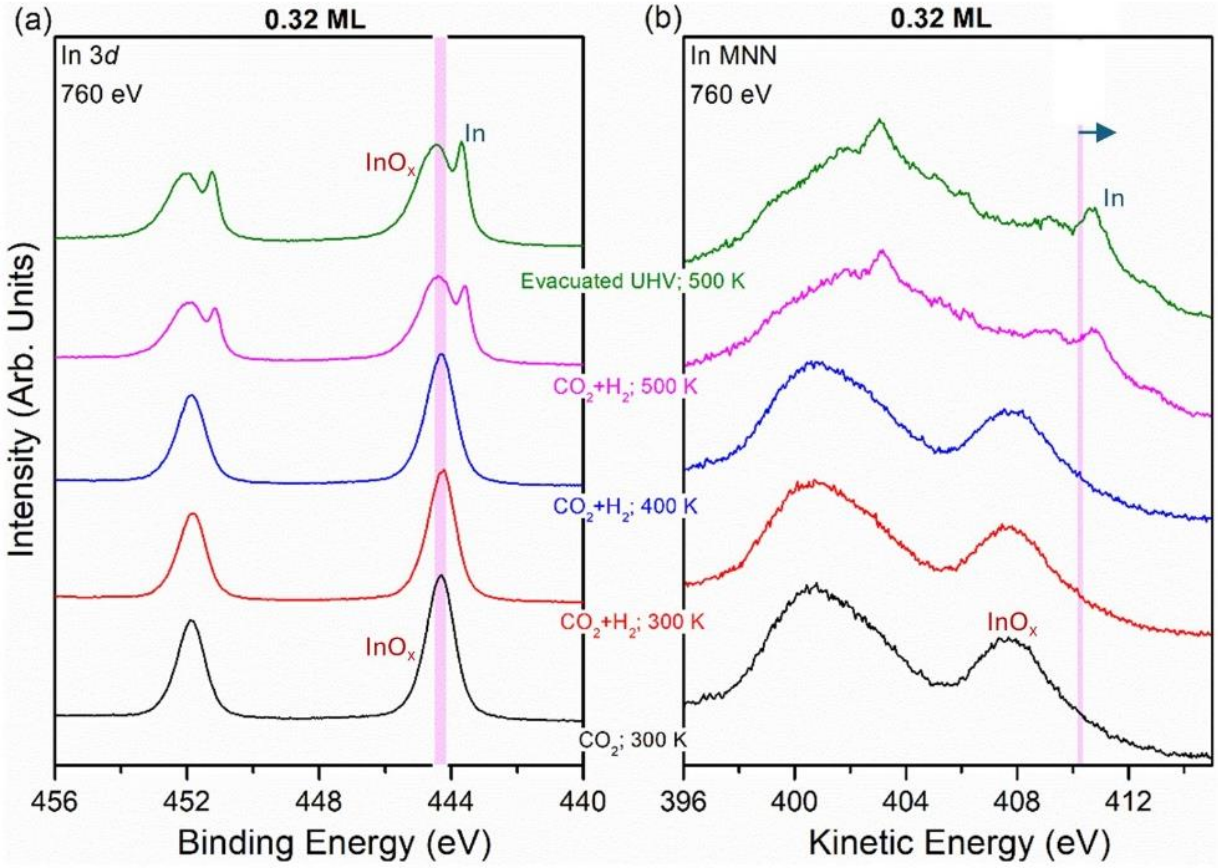


**Figure 8.** AP-XPS spectra of the (a) In 3*d* and (b) In MNN regions for a 0.32 ML of $InO_x/Cu_xO/Cu(111)$ surface under 250 mTorr of $CO_2$ + 750 mTorr of $H_2$ at various temperatures. In preliminary steps, the sample was initially reduced in $H_2$ at 400 K for 10 minutes (Figure 3) and after that treated with $CO_2$ at various temperatures (Figure S5).

The C 1s region of the 0.035 ML In coverage (bottom of Figure 9) shows prominent peaks for C* (284.1 eV) and $CH_x^*$ (285.0 eV), along with small signals for $CH_3O$* (287.1 eV) and $CO_3$*

(289.5 eV).[30,42-47] The corresponding O 1*s* spectra reveals the presence of $Cu_xO$, $InO_x$, and a set of $CO_x$ and $CHO_x$ species. Similar to the 0.32 ML $InO_x$ coverage, the addition of 750 mTorr of $H_2$ to the 0.035 ML $InO_x/Cu_xO/Cu(111)$ surface at room temperature leads to the formation of more C* (284.2 eV), $CH_x$ (285 eV), $CH_3O$ (287 eV), $CO_2^{\delta-}$, and $CO_3^{2-}$ species in the C and O 1*s* regions. However, the C*/Cu features decreased. No changes were seen in the In 3*d*, In MNN and Cu 2*p* spectrum.

Raising the temperature to 400 K led to an increase in $CH_x$ species. At the same time, $CH_3O$, $CO_2^{\delta-}$, and $CO_3^{2-}$ species decreased in intensity. Further raising the temperature to 500 K resulted in the complete reduction of both $InO_x$ and $Cu_xO$ (Figures S15 and S16). The complete disappearance of O 1*s* spectra further confirms the reduction of both $InO_x$, and $Cu_xO$ (Figure 9b, top). Thus, we are dealing with a dynamic $InO_x$-Cu interface that at high temperatures, when the synthesis of methanol occurs, transforms into a In-Cu(111) alloy. At 500 K, adsorbed C* is a dominant species along with $CH_x$ on the In-Cu surface. After comparing the two coverages, the 0.035 ML produced more C* species than the 0.32 ML by dissociating more C=O bonds in $CO_2$ gas. In contrast, the 0.32 ML surface formed more carbonate and formate species than the 0.035 ML. Nonetheless, both coverages followed a similar trend in $CO_2$ adsorption and hydrogenation.

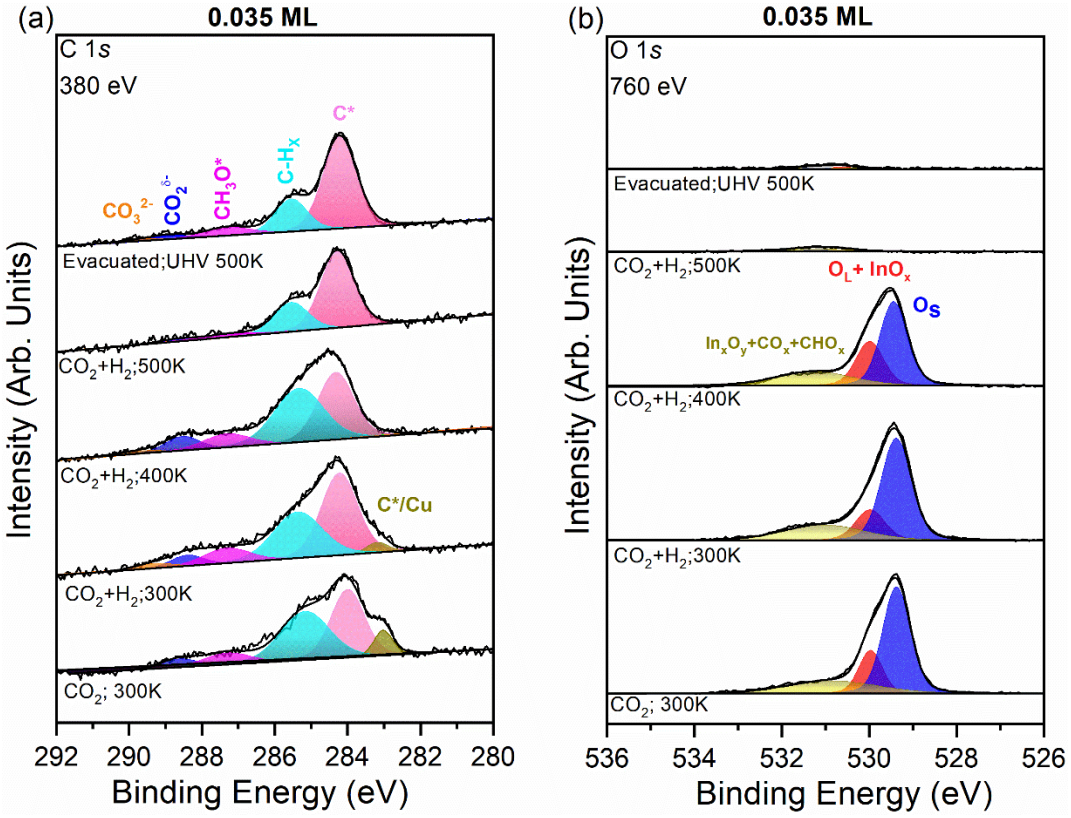

**Figure 9.** AP-XPS spectra of (a) the C 1*s* and (b) O 1*s* core levels of a 0.035 ML of $InO_x/Cu_xO/Cu(111)$ surface under 250 mTorr of $CO_2$ and 750 mTorr of $H_2$ at various temperatures. In preliminary steps, the sample was initially reduced in $H_2$ at 400 K for 10 minutes (Figure 3) and after that treated with $CO_2$ at various temperatures (Figure 6).

## Discussion

### A. Reactivity of $InO_x$-Cu(111) interfaces towards $CO_2$.

An important parameter to consider when dealing with an efficient $CO_2 \rightarrow CH_3OH$ conversion is the intrinsic reactivity of the oxide-metal interface towards $CO_2$. The non-polar nature and the high stability of $CO_2$ make the activation of this molecule difficult on surfaces of late transition or noble metals.[48-50] For example, in DFT studies, the binding energy of $CO_2$ on a flat or perfect Cu(111) surface is extremely small.[48-49, 51] This prediction has been corroborated by previous AP-XPS results which show that the molecule interacts weakly with Cu(111) and partial dissociation ($CO_{2,gas} \rightarrow O_{ads} + CO_{gas}$) is only observed when the density of steps and surface defects is high.[52-53] Our AP-XPS studies show that the addition of $InO_x$ to Cu(111) produces oxide-metal interfaces that have no problem binding and dissociating $CO_2$ at room temperature. In fact, these $InO_x$-Cu interfaces are also much more chemically active than bulk $In_2O_{3-x}$ where the predominant product for the adsorption of $CO_2$ are carbonate species.[30] Here, copper surfaces with small and medium coverages of $InO_x$ were able to fully dissociate $CO_2$ at room temperature and the adsorbed species reacted with $H_2$ from the background to yield methoxy (a key intermediate in $CH_3OH$ synthesis)[8] and $CH_x$ species. Theoretical calculations have shown substantial electronic perturbations in the oxide and metal components after forming $InO_x$-Cu(111) interfaces.[54] These electronic perturbations could enhance the reactivity of copper and $InO_x$ towards $CO_2$. On the other hand, in an oxide-metal interface, centers located in the indium oxide and copper could work in a cooperative way during the binding and transformation of $CO_2$.[55] The qualitative trends shown in our AP-XPS results agree with the fact that $Cu/In_2O_3$ catalysts exhibits good activity and excellent $CH_3OH$ selectivity (~ 90%) in $CO_2$ hydrogenation.[13] Overall, our studies highlight the promotional effects of $In_2O_3$ in enhancing the reactivity of Cu surfaces for $CO_2$ hydrogenation

### B. Dynamic formation of an In-Cu(111) alloy under $CO_2$ hydrogenation

A very interesting finding in our studies is the dynamic character of the $InO_x$-Cu interface as a function of temperature and reaction conditions, Figure 10. At low temperature (< 400K), $CO_2$ can oxidize an In-Cu alloy, but the formed $InO_x$ is not stable at high temperatures (> 500 K) under a

hydrogen rich atmosphere. In the case of a low coverage of InOx (< 0.05 ML), we saw complete transformations of $InO_x$/Cu into an In-Cu alloy (Figure 9b and S12). On the other hand, for a

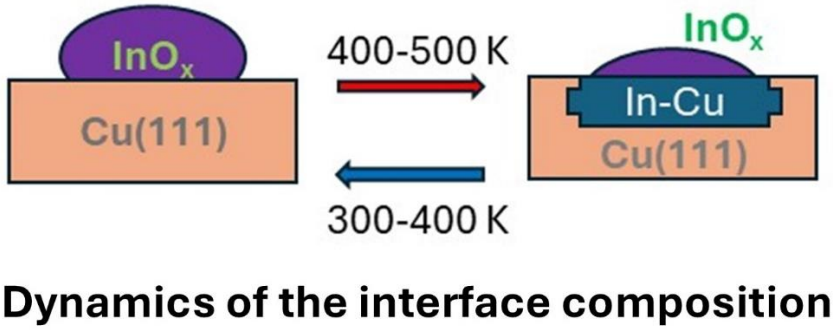


**Figure 10.** Scheme showing changes in the composition of the interface under an atmosphere of $CO_2/H_2$ at different temperatures. At medium temperatures (< 400 K), the In-Cu alloy can be oxidized by reaction with $CO_2$, but at high temperature (> 400 K), the $InO_x$ is reduced by hydrogen. The extent of the $InO_x$ reduction depends on the coverage of the oxide overlayer.

sizable coverage of $InO_x$, only a fraction of the oxide was reduced by hydrogen at high temperature (Figure 8). The stability of an $InO_x$ nanoparticle under hydrogen probably depends on its size: The larger the particle, the more stable it is. This basic principle could explain the trends seen in Figures 7-9 and S12. But, copper is far from being an innocent support.[54] It may interact strongly with the $InO_x$ to facilitate the dissociation of $H_2$[29,54] or form a stable alloy with In.[54] Both phenomena could facilitate the reduction of $InO_x$. In contrast, after depositing 0.3 ML of $InO_x$ on Au(111), there was no full reduction of the oxide at 500 K under a $CO_2/H_2$ atmosphere,[30] while partial reduction was observed in the case of $InO_x$/Cu(111) (Figures 7b and 8). Overall, the $CO_2$ hydrogenation process on a pre-reduced $InO_x$-Cu interface could be seen as a redox process,[56-57]where $CO_2$ oxidizes the active sites in a first step, and then hydrogen reduces them in subsequent steps.

The XPS studies described above clearly point to dynamic changes in the composition of the $InO_x$-Cu interface as a function of temperature and chemical environment around the sample. To fully understand this phenomenon, future research must be done to investigate the associated structural and morphological changes. A static view of the $InO_x$-Cu interface is not valid. The XPS results show variations in composition and chemical reactivity that deserve more attention due to their relevance for catalytic processes.

## Conclusions

In summary, we deposited small and medium coverages of indium oxide on a $Cu_xO$/Cu(111) substrate and, after pre-reduction in $H_2$, investigated their ability to adsorb and hydrogenate $CO_2$ using synchrotron-based AP-XPS. Our finding indicates that the $InO_x$-Cu(111) interfaces effectively adsorb and activate $CO_2$ at room temperature. Photoemission studies revealed that during $CO_2$ hydrogenation, a surface with 0.035 ML of $In_2O_3$ on Cu(111) undergoes chemical changes at/above 500 K, forming a In-Cu(111) alloy. An increase in indium coverage (0.32 ML) resulted in a $InO_x$/Cu(111) system that was only partially reduced at high temperature, where $InO_x$ and an In-Cu alloy coexisted at the interface. Reaction mechanistic studies showed that surface bound species like C*, $CH_x$, $CH_3O$, $CO_2^{\delta-}$, and $CO_3^{2-}$ formed under $CO_2$ adsorption and hydrogenation conditions. These species were not observed on a bare Cu(111) surface. Overall, our results clearly demonstrate the promotional effects of $In_2O_{3-x}$ for enhancing the reactivity of Cu surfaces for $CO_2$ hydrogenation and the dynamic character of the $InO_x$-Cu interface as a function of temperature and chemical environment.

## Supporting Information

XPS and Auger spectra for the characterization of $InO_x$/$Cu_xO$/Cu(111) surfaces and their reaction with $CO_2$, $H_2$ and $CO_2$/$H_2$ mixtures.

## Acknowledgements

The research done at the Chemistry Division of Brookhaven National Laboratory was supported by the U.S. Department of Energy, Office of Science, Office of Basic Energy Sciences, Chemical Sciences, Geosciences, and Biosciences Division, Catalysis Science Program (Grant No DE-SC0012704). This research used resources of the 23-ID-2 (IOS) beamline of the National Synchrotron Light Source II, a U.S. Department of Energy (DOE) Office of Science User Facility operated for the DOE Office of Science by Brookhaven National Laboratory under Contract No. DE-SC0012704.

## References

1. Anderson, T. R.; Hawkins, E.; Jones, P. D. $CO_2$, the Greenhouse Effect and Global Warming: from the Pioneering Work of Arrhenius and Callendar to Today's Earth System

Models. *Endeavour* **2016**, *40*, 178–187.
2. Bushuyev, O. S.; De Luna, P.; Dinh, C. T.; Tao, L.; Saur, G.; van de Lagemaat, J.; Kelley, S. O.; Sargent, E. H. What Should We Make with $CO_2$ and How Can We Make It? *Joule* **2018**, *2*, 825–832.
3. Jones, W. D. Carbon Capture and Conversion. *J. Am. Chem. Soc.* **2020**, *142*, 4955– 4957.
4. Verhelst, S.; Turner, J. W.; Sileghem, L.; Vancoillie, J. Methanol as a Fuel for Internal Combustion Engines. *Prog. Energy Combust. Sci.* **2019**, *70*, 43–88.
5. Olah, G. A. Beyond Oil and Gas: the Methanol Economy. *Angew. Chem., Int. Ed.* **2005**, *44*, 2636–2639.
6. Ott, J.; Gronemann, V.; Pontzen, F.; Fiedler, E.; Grossman, G.; Burkhard Kersebohm, K.; Weiss, G.; Witte, C. Methanol - An Industrial Review. *Ullmann's Encyclopedia of Industrial Chemistry*; Wiley-VCH Verlag GmbH & Co. KGaA, **2012**.
7. Shindell, D.; Borgford-Parnell, N.; Brauer, M.; Haines, A.; Kuylenstierna, J. C. I.; Leonard, S. A.; Ramanathan, V.; Ravishankara, A.; Amann, M.; Srivastava, L. A climate policy pathway for near- and long-term benefits. *Science* **2017**, *356*, 493–494.
8. Jianyang, W.; Zhang, G.; Zhu, J.; Xinbao, Z.; Ding, F.; Zhang, A.; Guo, X.; Song, C. $CO_2$ Hydrogenation to Methanol over $In_2O_3$-Based Catalysts: From Mechanism to Catalyst Development. *ACS Catal.* **2021**, *11*, 1406–1423.
9. Wang, W.; Huo, K.; Wang, Y.; Xie, J.; Sun, X.; He, Y.; Li, M.; Liang, J.; Gao, X. Rational Control of Oxygen Vacancy Density in $In_2O_3$ to Boost Methanol Synthesis from $CO_2$ Hydrogenation. *ACS Catal.* **2024**, *14*, 9887–9900.
10. Cao, A.; Wang, Z.; Li, H.; Nørskov, J. K. Relations between surface oxygen vacancies and activity of methanol formation from $CO_2$ hydrogenation over $In_2O_3$ surfaces. *ACS Catal.* **2021**, *11*, 1780–1786.
11. Rui, N.; Zhang, F.; Sun, K.; Liu, Z.; Xu, W.; Stavitski, E.; Senanayake, S. D.; Rodriguez, J. A.; Liu, C.-J. Hydrogenation of $CO_2$ to Methanol on a $Au^{\delta+}$-$In_2O_{3-x}$ Catalyst. *ACS Catal.* **2020**, *10*, 11307–11317.
12. Rui, N.; Wang, X.; Deng, K.; Moncada, J.; Rosales, R.; Zhang, F.; Xu, W.; Waluyo, I.; Hunt, A.; Stavitski, E.; Senanayake, S. D.; Liu, P.; Rodriguez, J. A. Atomic structural origin of the high methanol selectivity over $In_2O_3$-metal interfaces: metal-support interactions and the formation of a $InO_x$ overlayer in $Ru/In_2O_3$ catalysts during $CO_2$ hydrogenation. *ACS Catal.* **2023**, *13*, 3187–3200.
13. Xie, S.; Luo, X.; Zhao, J.; Xu, M.; Chen, H.; Zhu, M.; Xu, J. Synergistic Effect of Copper and Indium Species for Highly Selective $CO_2$ Hydrogenation to Methanol. *ACS Sustainable Chem. Eng.* **2024**, *12*, 17925–17935.
14. Zhong, Z.; Etim, U. J.; Song, Y. Improving the Cu/ZnO-Based Catalysts for Carbon Dioxide Hydrogenation to Methanol, and the Use of Methanol as a Renewable Energy Storage Media. *Front. Energy Res.* **2020**, *8*, 545431.
15. Shi, Z.; Tan, Q.; Tian, C.; Pan, Y.; Sun, X.; Zhang, J.; Wu, D. $CO_2$ hydrogenation to methanol over Cu-In intermetallic catalysts: Effect of reduction temperature. *J.*

*Catal.* **2019**, *379*, 78–89.
16. Shi, Z.; Pan, M.; Wei, X.; Wu, D. Cu-In intermetallic compounds as highly active catalysts for $CH_3OH$ formation from $CO_2$ hydrogenation. *Int. J. Energy Res.* **2022**, *46*, 1285–1298.
17. Li, M.; Luo, W.; Züttel, A. Near ambient-pressure X-ray photoelectron spectroscopy study of $CO_2$ activation and hydrogenation on indium/copper surface. *J. Catal.* **2021**, *395*, 315–324.
18. Kapiamba, K. F.; Otor, H. O.; Viamajala, S.; Alba-Rubio, A. C. Inverse oxide/metal catalysts for $CO_2$ hydrogenation to methanol. *Energy Fuels* **2022**, *36*, 11691–11711.
19. Kordus, D.; Widrinna, S.; Timoshenko, J.; Lopez Luna, M.; Rettenmaier, C.; Chee, S. W.; Ortega, E.; Karslioglu, O.; Kühl, S.; Roldan Cuenya, B. Enhanced Methanol Synthesis from $CO_2$ Hydrogenation Achieved by Tuning the Cu-ZnO Interaction in ZnO/$Cu_2O$ Nanocube Catalysts Supported on $ZrO_2$ and $SiO_2$. *J. Am. Chem. Soc.* **2024**, *146*, 8677– 8687.
20. Zhang, F. X.; Li, B. Y.; Quan, X.; Wang, K.; Xu, J. Y.; Wu, T. T.; Li, Z. L.; Yan, M.; Liu, S. J.; He, Y.; Shi, Y.; Su, Y. Q.; Xie, P. F. Revealing the Dynamics of Oxygen Vacancy in $ZnO_{1-x}$/Cu during Robust Methanol Synthesis from $CO_2$. *ACS Catal.* **2024**, *14*, 7136– 7148.
21. Liu, X.; Luo, J.; Wang, H.; Huang, L.; Wang, S.; Li, S.; Sun, Z.; Sun, F.; Jiang, Z.; Wei, S.; Li, W.-X.; Lu, J. In situ spectroscopic characterization and theoretical calculations identify partially reduced $ZnO_{1-x}$/Cu interfaces for methanol synthesis from $CO_2$. *Angew. Chem. Inter. Ed.* **2022**, *61*, e202202330.
22. Zhang, J.; Medlin, J. W. Catalyst design using an inverse strategy: From mechanistic studies on inverted model catalysts to applications of oxide-coated metal nanoparticles. *Surf. Sci. Rep.* **2018**, *73*, 117–152.
23. Rodriguez, J. A.; Liu, P.; Graciani, J.; Senanayake, S. D.; Grinter, D. C.; Stacchiola, D.; Hrbek, J.; Fernández-Sanz, J. Inverse Oxide/Metal Catalysts in Fundamental Studies and Practical Applications: A Perspective of Recent Developments. *J. Phys. Chem. Lett.* **2016**, *7*, 2627–2639.
24. Lunkenbein, T.; Schumann, J.; Behrens, M.; Schlögl, R.; Willinger, M. G. Formation of a ZnO Overlayer in Industrial Cu/ZnO/$Al_2O_3$ Catalysts Induced by Strong Metal-Support Interactions. *Angew. Chem., Int. Ed.* **2015**, *54*, 4544–4548.
25. Palomino, R. M.; Ramírez, P. J.; Liu, Z.; Hamlyn, R.; Waluyo, I.; Mahapatra, M.; Orozco, I.; Hunt, A.; Simonovis, J. P.; Senanayake, S. D.; Rodriguez, J. A. Hydrogenation of $CO_2$ on ZnO/Cu (100) and ZnO/Cu (111) catalysts: role of copper structure and metal–oxide interface in methanol synthesis. *J. Phys. Chem. B* **2018**, *122*, 794–800.
26. Kattel, S.; Ramirez, P. J.; Chen, J. G.; Rodriguez, J. A.; Liu, P. Active Sites for $CO_2$ Hydrogenation to Methanol on Cu/ZnO Catalysts. *Science* **2017**, *355*, 1296–1299.
27. Mahapatra, M.; Kang, J.; Ramírez, P. J.; Hamlyn, R.; Rui, N.; Liu, Z.; Orozco, I.; Senanayake, S. D.; Rodriguez, J. A. G. Growth, Structure, and Catalytic Properties of $ZnO_x$ Grown on $CuO_x$/Cu(111) Surfaces. *J. Phys. Chem. C* **2018**, *122* (46), 26554–26562.
28. Waluyo, I.; Hunt, A. Ambient Pressure X-Ray Photoelectron Spectroscopy at the IOS (23-ID-2) Beamline at the National Synchrotron Light Source II. *Synchrotron Radiat. News* **2022**, *35*, 31–38.
29. Mehar, V.; Huang, E.; Shi, R.; Rosales, R.; Waluyo, I.; Hunt, A.; Liu, P.; Rodriguez, J.

A. Microscopic Investigation of $H_2$ Reduced $CuO_x$/Cu(100) and ZnO/$CuO_x$/Cu(111) Inverse Catalysts: STM AP-XPS, and DFT Studies. *ACS Catal.* **2023**, *13*, 9857–9870.
30. Reddy, K. P.; Tian, Y.; Ramirez, P. J.; Islam, A.; Lim, H.; Rui, N.; Xie, Y.; Hunt, A.; Waluyo, I.; Rodriguez, J. A. Insights into the Surface Electronic Structure and Catalytic Activity of $InO_x$/Au(111) Inverse Catalysts for $CO_2$ Hydrogenation to Methanol. *ACS Catal.* **2024**, *14*, 17148–17158.
31. Zou, R.; Shen, C.; Sun, K.; Ma, X.; Li, Z.; Li, M.; Liu, C.-J. $CO_2$ hydrogenation to methanol over the copper promoted $In_2O_3$ catalyst. *J. Energy Chem.* **2024**, *93*, 135–145.
32. Yang, Y.; Wu, L.; Bingqing, Y.; Zhang, L.; Jung, M.; He, Q.; Yan, N.; Liu, C.-J. Gallium Cluster-Promoted $In_2O_3$ Catalyst for $CO_2$ Hydrogenation to Methanol. *ACS Catal.* **2024**, *14*, 13958–13972.
33. Roy, K.; Gopinath, C. S. UV Photoelectron Spectroscopy at Near Ambient Pressures: Mapping Valence Band Electronic Structure Changes from Cu to CuO. *Anal. Chem.* **2014**, *86*, 3683–3687.
34. Wang, J.; Li, R.; Zhang, G.; Dong, C.; Fan, Y.; Yang, S.; Chen, M.; Guo, X.; Mu, R.; Ning, Y.; Li, M.; Fu, Q.; Bao, X. Confinement-Induced Indium Oxide Nanolayers Formed on Oxide Support for Enhanced $CO_2$ Hydrogenation Reaction. *J. Am. Chem. Soc.* **2024**, *146*, 5523–5531.
35. Reddy, K. P.; Islam, A.; Tian, Y.; Lim, H.; Kim, J.; Kim, D.; Hunt, A.; Waluyo, I.; Rodriguez, J. A. MgO Nanostructures on Cu(111): Understanding Size- and Morphology-Dependent $CO_2$ Binding and Hydrogenation. *J. Phys. Chem. C* **2024**, *128*, 7149–7158.
36. Lv, J.; Sun, H.; Liu, G.; Liu, T.; Zhao, G.; Wang, Y.; Tu, X.; Yan, Z. Rational Design of Indium–Palladium Intermetallic Catalysts for Selective $CO_2$ Hydrogenation to Methanol. *ACS Catal.* **2025**, *15*, 1, 23–33.
37. Graciani, J; Mudiyanselage, K.; Xu, F.; Baber, A.E.; Evans, J.; Senanayake, S.D.; Stacchiola, D.J.; Liu, P.; Hrbek, J.; Fernandez Sanz, J.; Rodriguez, J. A. Highly Active Copper-Ceria Titania Catalysts for Methanol Synthesis from $CO_2$, *Science*, **2014**, *345*, 546-551.
38. Moncada, J.; Chen, X.; Deng, K.; Wang, Y.; Xu, W.; Marinkovic, N.; Zhou, G.; Martinez-Arias, A.; Rodriguez, J. A. Structural and Chemical Evolution of an Inverse $CeO_x$/Cu Catalyst under $CO_2$ Hydrogenation, *ACS Catal.* **2023**, *13*, 15248-15258.
39. Cordfunke, E. H. P.; Konings, R. J. M.; Ouweltjes, W. The Standard Enthalpy of Formation of $In_2O_3$. *J. Chem. Thermodyn.* **1991**, *23*, 451–454.
40. Linstrom, P. J.; Mallard, W. G., Eds. NIST Chemistry WebBook; NIST Standard Reference Database Number 69; National Institute of Standards and Technology: Gaithersburg, MD, **2011**. http://webbook.nist.gov.
41. Idriss, H. On the Wrong Assignment of the XPS O1s Signal at 531–532 eV Attributed to Oxygen Vacancies in Photo- and Electro-Catalysts for Water Splitting and Other Materials Applications. *Surf. Sci.* **2021**, *712*, 121894.

42. Sock, M.; Eichler, A.; Surnev, S.; Andersen, J. N.; Klötzer, B.; Hayek, K.; Ramsey, M. G.; Netzer, F. P. High-resolution electron spectroscopy of different adsorption states of ethylene on Pd(111). *Surf. Sci.* **2003**, *545*, 122–136.
43. Mullins, D. R. The Surface Chemistry of Cerium Oxide. *Surf. Sci. Rep.* **2015**, *70*, 42–85.
44. Deng, X.; Verdaguer, A.; Herranz, T.; Weis, C.; Bluhm, H.; Salmeron, M. Surface chemistry of Cu in the presence of $CO_2$ and $H_2O$. *Langmuir* **2008**, *24*, 9474–9478.
45. Gamba, O.; Hulva, J.; Pavelec, J.; Bliem, R.; Schmid, M.; Diebold, U.; Parkinson, G. S. The Role of Surface Defects in the Adsorption of Methanol on $Fe_3O_4$(001). *Top. Catal.* **2017**, *60*, 420– 430
46. Tanaka, K.; Matsuzaki, S.; Toyoshima, I. Photodecomposition of Adsorbed Methoxy Species by UV-Light and Formaldehyde Adsorption on Si(111) Studied by XPS And UPS. *J. Phys. Chem.* **1993**, *97*, 5673–5677.
47. Mullins, D. R.; Robbins, M. D.; Zhou, J. Adsorption and Reaction of Methanol on Thin-film Cerium Oxide. *Surf. Sci.* **2006**, *600*, 1547–1558.
48. Jin, W.; Wang, Y.; Liu, T.; Ding, C.; Guo, H. $CO_2$ Chemisorption and Dissociation on Flat and Stepped Transition Metal Surfaces. *Appl. Surf. Sci.* **2022**, *599*, 154024.
49. Liu, X.; Sun, L.; Deng, W.-Q. Theoretical Investigation of $CO_2$ Adsorption and Dissociation on Low Index Surfaces of Transition Metals. *J. Phys. Chem. C* **2018**, *122*, 8306–8314.
50. Freund, H. J.; Roberts, M. W. Surface chemistry of carbon dioxide. *Surf. Sci. Rep.* **1996**, *25*, 225–273.
51. Yang, Y.; Evans, J.; Rodriguez, J. A.; White, M. G.; Liu, P. Fundamental studies of methanol synthesis from $CO_2$ hydrogenation on Cu(111), Cu clusters, and Cu/ZnO(0001). *Phys. Chem. Chem. Phys.* **2010**, *12*, 9909–9917.
52. Eren, B.; Weatherup, R. S.; Liakakos, N.; Somorjai, G. A.; Salmeron, M. Dissociative Carbon Dioxide Adsorption and Morphological Changes on Cu(100) and Cu(111) at Ambient Pressures. *J. Am. Chem. Soc.* **2016**, *138*, 8207–8211.
53. Hagman, B.; Posada-Borbon, A.; Schaefer, A.; Shipilin, M.; Zhang, C.; Merte, L. R.; Hellman, A.; Lundgreen, E.; Grönbeck, H.; Gustafson, J. Steps Control the Dissociation of $CO_2$ on Cu(100). *J. Am. Chem. Soc.* **2018**, *140*, 12974–12979.
54. Kempen, L.H.E., Andersen, M. Inverse catalysts: tuning the composition and structure of oxide clusters through the metal support. *npj Comput Mater* **2025,** *11*, 8.
55. Grinter, D. C.; Graciani, J.; Palomino, R. M.; Xu, F.; Waluyo, I.; Fdez Sanz, J.; Senanayake, S. D.; Rodriguez, J. A. Adsorption and Activation of $CO_2$ on Pt/CeOx/$TiO_2$(110): Role of the Pt-$CeO_x$ Interface. *Surf. Sci.* **2021**, *710*, 121852.
56. Mehar, V.; Kim, J.; Hunt, A.; Waluyo, I.; Rodriguez, J. A. AP-XPS Study of the Reaction of $O_2$ and $CO_2$ with Zn-Au(111) Alloys: Activation of O–O/C–O Bonds and the Formation of ZnO. *J. Phys. Chem. C* **2024**, *128*, 13852–13863.
57. Docherty, S. R.; Safonova, O. V.; Copéret, C. Surface Redox Dynamics in Gold–Zinc $CO_2$ Hydrogenation Catalysts. *J. Am. Chem. Soc.* **2023**, *145*, 13526–13530.

**TOC**

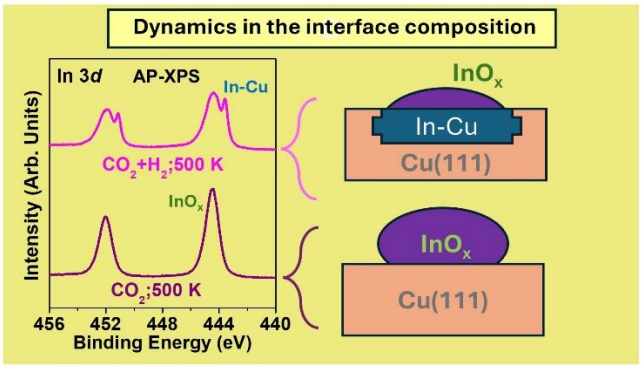
Dynamics in the interface composition
In 3d AP-XPS
In-Cu
CO2+H2;500 K
InOx
CO2;500 K
Intensity (Arb. Units)
456 452 448 444 440
Binding Energy (eV)
InOx
In-Cu
Cu(111)
InOx
Cu(111)